




Superradiant atomic recoil lasing with orbital-angular-momentum light

A. T. Gisbert and N. Piovella *Dipartimento di Fisica “Aldo Pontremoli,” Università degli Studi di Milano, Via Celoria 16, I-20133 Milano, Italy*G. R. M. Robb  and D. G. McLellan *SUPA and Department of Physics, University of Strathclyde, Glasgow G4 0NG, Scotland, United Kingdom*

(Received 5 November 2021; accepted 9 February 2022; published 25 February 2022)

We analyze the collective light scattering by cold atoms in free space of a pump-laser beam possessing orbital angular momentum. We derive a set of coupled multiparticle equations for the atomic motion in which the vacuum-mode field is adiabatically eliminated. The resulting equations describe collective recoil as due to either transfer of linear momentum or orbital angular momentum. For a transverse annular atomic distribution the initial equilibrium with uniform atomic phases and no scattered field is unstable. The atoms are set in rotation and bunched in phase at different harmonics depending on the pump azimuthal index ℓ and on the ring radius.

DOI: [10.1103/PhysRevA.105.023526](https://doi.org/10.1103/PhysRevA.105.023526)

I. INTRODUCTION

Optomechanical collective effects in cold atomic systems, where atomic density structures and optical fields evolve simultaneously under their mutual influence, have been a topic of interest for several years now. In particular, the exchange of (linear) momentum between the photons of an incident optical pump and those of a back-scattered field in an optical ring cavity has led to the concept of the collective atomic recoil laser (CARL), predicted in the 1990's [1,2] and subsequently experimentally observed [3,4]. It is well known that light may carry also spin angular momentum (SAM) [5] and orbital angular momentum (OAM) [6] in addition to linear momentum. Transfer of OAM from light to atoms was first studied theoretically in [7], and has been studied extensively ever since [8]. The idea of an analogous effect to CARL involving collective exchange of OAM between a pump and a scattered field was proposed in [9,10]. In this scheme, two copropagating, counter-rotating Laguerre-Gaussian beams incident on a gas of ultracold atoms give rise to a superradiant instability in which orbital angular momentum is transferred to the atoms and the probe field is amplified. The atoms acquire angular momentum in discrete amounts of $2\ell\hbar$, where ℓ is the magnitude of the azimuthal index of the Laguerre-Gaussian beams. The instability involves the development of an azimuthal density modulation in the atomic distribution. Since the pump and probe beams are copropagating, no net exchange of linear momentum occurs in the scattering process. Similar theoretical studies of superradiant scattering into radially propagating end-fire modes from a pancake shaped Bose-Einstein condensate (BEC) were performed in [11,12], where the production of vortices in the BEC was predicted as a consequence of the superradiant scattering process.

Recently, a multimode theory of CARL in free space has been developed [13,14], where no assumption about the scattered direction was made. Contrary to the usual CARL phenomena, where the light scattering occurs effectively in

a single spatial mode defined by the axis of a ring cavity or the major axis of an elongated atomic sample, in free space the pump photons are initially scattered into the three-dimensional (3D) vacuum modes, and only at later times the dominant modes of the scattered light emerge naturally from the collective process.

In this paper, we extend the multimode CARL theory for a pump laser consisting of a hollow Laguerre-Gaussian beam with azimuthal index ℓ , without any assumption about the scattered field. The model leads to a set of coupled equations for the atoms in which the scattered field is adiabatically eliminated. This model describes a superradiant emission process involving exchange of either linear momentum, in units of $\mathbf{p} = \hbar\mathbf{k}$, or OAM, in units of $\hbar\ell$. In particular, we investigate the dynamics of the atomic motion for an annular transverse distribution in which the longitudinal motion along the pump direction is neglected. We find that the initial equilibrium, with atoms uniformly distributed along the ring and no scattered photons, is unstable. The atoms are set in rotation and bunched in phase by a collective process, emitting a field with a transverse pattern distribution depending on the azimuthal index ℓ and on the ring radius.

The paper is organized as follows. In Sec. II we present the theoretical model, starting from the Hamiltonian of N two-level atoms interacting with the OAM pump and the vacuum-mode field. We derive from it the single-atom forces, the OAM-CARL multimode equations, the superradiant equations describing the 3D atomic motion, and the scattered field. In Sec. III we consider the motion in a transverse plane neglecting the longitudinal motion. Section IV further reduces the atomic motion to the case where the atoms are trapped in a thin circular ring. In Sec. V we address the one-dimensional dynamics of the atoms in a ring, calculating the equilibrium and the linear stability. Numerical results for the nonlinear evolution are presented in Sec. VI and conclusions are drawn in Sec. VII.

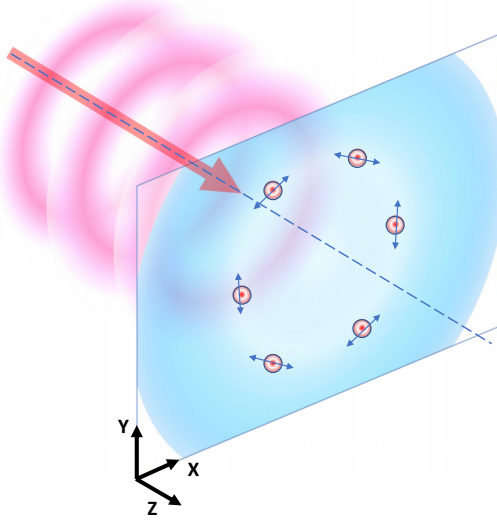


FIG. 1. Schematic of the experimental setup. The pump beam is incident along the z axis on an annular atomic distribution.

II. MODEL

A schematic representation of the setup is shown in Fig. 1. It consists of a collection of cold atoms in an annular configuration [15,16] in the plane (x, y) , upon which a pump field consisting of a Laguerre-Gaussian mode is incident along the z direction. The atoms scatter the incident photon in all 3D directions. In the following we introduce the equations describing the evolution of the center of mass of each atom under the optical dipole force of the pump and scattered field, and of the multimode scattered field. In free space the optical field can be adiabatically eliminated, leading to a set of coupled equations for the atoms.

A. OAM pump field

We assume a pump consisting of a hollow Laguerre-Gaussian mode $LG_{0\ell}$ directed along the z axis and linearly polarized, the electric-field component of which, expressed in cylindrical coordinates, has the form [17]

$$E_0(\rho, \phi, z) = A_0 R(\rho) e^{i(k_0 z + \ell \phi - \omega_0 t)} + \text{c.c.} \quad (1)$$

We assume, without loss of generality, $\ell > 0$, and define

$$R(\rho) = e^{-\rho^2/w^2} \left(\frac{\sqrt{2}\rho}{w} \right)^\ell, \quad (2)$$

$$A_0 = \sqrt{\frac{2^{\ell+1} P_0}{\pi w^2 \ell! \epsilon_0 c}}, \quad (3)$$

where w is the beam waist (assumed constant) and P_0 is the mode power.

B. Hamiltonian

We assume N two-level atoms with internal states $|g_j\rangle$ and $|e_j\rangle$, with positions and momenta \mathbf{r}_j and $\mathbf{p}_j = M\mathbf{v}_j$ (with $j = 1, \dots, N$), mass M , resonant frequency ω_a , and dipole d , interacting with a pump OAM field given by Eq. (1) and

scattering photons in the vacuum modes with wave number \mathbf{k} and frequency ω_k . The system is described by the Hamiltonian

$$H = H_L + H_V. \quad (4)$$

The first term of Eq. (4) describes the interaction of the atoms with the pump laser, with

$$H_L = \sum_{j=1}^N \frac{\mathbf{p}_j^2}{2M} + \frac{\hbar\Omega_0}{2} \sum_{j=1}^N R(\rho_j) [\sigma_j^- e^{i\Delta_0 t - ik_0 z_j - i\ell\phi_j} + \sigma_j^+ e^{-i\Delta_0 t + ik_0 z_j + i\ell\phi_j}], \quad (5)$$

where $\Omega_0 = dA_0/\hbar$ is the pump Rabi frequency and $\Delta_0 = \omega_0 - \omega_a$ is the pump-atom detuning. The internal dynamics of the two-level atoms are described by the operators $\sigma_j^z = |e_j\rangle\langle e_j| - |g_j\rangle\langle g_j|$, $\sigma_j^+ = |e_j\rangle\langle g_j|$, and $\sigma_j^- = |g_j\rangle\langle e_j|$. The second term of Eq. (4) describes the interaction between the atoms and the vacuum-mode field, with

$$H_V = \hbar \sum_{\mathbf{k}} g_{\mathbf{k}} [a_{\mathbf{k}}^\dagger \sigma_j^- e^{i\Delta_{\mathbf{k}} t - i\mathbf{k}\cdot\mathbf{r}_j} + \sigma_j^+ a_{\mathbf{k}} e^{-i\Delta_{\mathbf{k}} t + i\mathbf{k}\cdot\mathbf{r}_j}]. \quad (6)$$

The vacuum modes, described by the operators $a_{\mathbf{k}}$, have wave vectors \mathbf{k} and frequency ω_k with $\Delta_k = \omega_k - \omega_a$, coupling rate $g_{\mathbf{k}} = d[\omega_k/(2\hbar\epsilon_0 V_{ph})]^{1/2}$, V_{ph} being the quantization volume. We disregard polarization and short-range effects, using a scalar model for the radiation field.

The Heisenberg equations for the dipole operators σ_j^- are

$$\dot{\sigma}_j^- = i \left[\frac{\Omega_0}{2} R(\rho_j) e^{-i\Delta_0 t + ik_0 z_j + i\ell\phi_j} + \sum_{\mathbf{k}} g_{\mathbf{k}} a_{\mathbf{k}} e^{-i\Delta_{\mathbf{k}} t + i\mathbf{k}\cdot\mathbf{r}_j} \right] \sigma_j^z. \quad (7)$$

Introducing $\sigma_j = \sigma_j^- e^{i\Delta_0 t}$ and neglecting the population of the excited state (assuming weak field and/or large detuning Δ_0), so that $\sigma_j^z \approx -1$,

$$\dot{\sigma}_j = \left(i\Delta_0 - \frac{\Gamma}{2} \right) \sigma_j - \frac{i\Omega_0}{2} R(\rho_j) e^{ik_0 z_j + i\ell\phi_j} - i \sum_{\mathbf{k}} g_{\mathbf{k}} a_{\mathbf{k}} e^{-i(\omega_k - \omega_0)t + i\mathbf{k}\cdot\mathbf{r}_j}, \quad (8)$$

where we added the spontaneous emission decay term $-(\Gamma/2)\sigma_j$, with $\Gamma = d^2 k^3 / 2\pi\epsilon_0 \hbar$ as the spontaneous decay rate. Assuming $\Gamma \gg \omega_{\text{rec}}$, $\omega_{\text{rec}} = \hbar k^2 / 2M$ being the recoil frequency, we can adiabatically eliminate the internal degree of freedom, taking $\dot{\sigma}_j \approx 0$ in Eq. (8):

$$\sigma_j \approx \frac{1}{\Delta_0 + i\Gamma/2} \left[\frac{\Omega_0}{2} R(\rho_j) e^{ik_0 z_j + i\ell\phi_j} + \sum_{\mathbf{k}} g_{\mathbf{k}} a_{\mathbf{k}} e^{-i(\omega_k - \omega_0)t + i\mathbf{k}\cdot\mathbf{r}_j} \right]. \quad (9)$$

The first term describes the dipole excitation induced by the driving field, whereas the second term is the excitation induced by the scattered field.

C. Single-atom forces

The OAM laser beam induces on each atom a mechanical force

$$\mathbf{F}_{Lj} = -\nabla_j H_L = \mathbf{F}_{zj} + \mathbf{F}_{\phi j} + \mathbf{F}_{\rho j}, \quad (10)$$

the components of which can be derived using Eq. (5), assuming cylindrical coordinates and retaining only the first term of Eq. (9):

$$\mathbf{F}_{zj} = -\hat{\mathbf{u}}_z \frac{\partial H_L}{\partial z_j} = \hbar k_0 \frac{\Gamma}{\Delta_0^2 + \Gamma^2/4} \left[\frac{\Omega_0 R(\rho_j)}{2} \right]^2 \hat{\mathbf{u}}_z, \quad (11)$$

$$\mathbf{F}_{\phi j} = -\frac{\hat{\mathbf{u}}_\phi}{\rho_j} \frac{\partial H_L}{\partial \phi_j} = \ell \hbar \frac{\Gamma}{\Delta_0^2 + \Gamma^2/4} \left[\frac{\Omega_0 R(\rho_j)}{2} \right]^2 \frac{\hat{\mathbf{u}}_\phi}{\rho_j}, \quad (12)$$

$$\begin{aligned} \mathbf{F}_{\rho j} &= -\hat{\mathbf{u}}_\rho \frac{\partial H_L}{\partial \rho_j} = -\frac{2\hbar\Delta_0}{\Delta_0^2 + \Gamma^2/4} \left[\frac{\Omega_0 R(\rho_j)}{2} \right]^2 \\ &\times \left[\frac{\ell}{\rho_j} - \frac{2\rho_j}{w^2} \right] \hat{\mathbf{u}}_\rho. \end{aligned} \quad (13)$$

The force \mathbf{F}_{zj} is the usual radiation pressure force, directed along the incidence direction of the laser beam, with $\mathbf{k}_0 = k_0 \hat{\mathbf{u}}_z$. The azimuthal force $\mathbf{F}_{\phi j}$ produces a torque directed along the z axis, which put the atoms in rotation [7]. The radial force $\mathbf{F}_{\rho j}$ is zero for $\rho_j = w\sqrt{\ell/2}$ [where $R(\rho_j)$ is maximum] and is focusing toward this maximum for $\Delta_0 < 0$.

D. Multimode OAM-CARL model

Assuming the pump field detuning $\Delta_0 \gg \Gamma$, we neglect the multiple scattering processes. The resulting multimode equations describing the collective recoil in the presence of an OAM pump beam are (see Appendix A)

$$\dot{\mathbf{r}}_j = \frac{\mathbf{p}_j}{M}, \quad (14)$$

$$\begin{aligned} \dot{\mathbf{p}}_j &= i\hbar g R(\rho_j) \sum_{\mathbf{k}} (\mathbf{k}_0 - \mathbf{k}) \{ a_{\mathbf{k}} e^{-i(\mathbf{k}_0 - \mathbf{k}) \cdot \mathbf{r}_j - i\ell\phi_j - i\delta_k t} - \text{H.c.} \} \\ &- \hbar g \left\{ \left[\frac{dR(\rho_j)}{d\rho_j} \hat{\mathbf{u}}_\rho - i\ell \frac{R(\rho_j)}{\rho_j} \hat{\mathbf{u}}_\phi \right] \right\} \end{aligned}$$

$$\dot{\mathbf{r}}_j = \frac{\mathbf{p}_j}{M}, \quad (18)$$

$$\begin{aligned} \dot{\mathbf{p}}_j &= \Gamma \hbar k_0 \left(\frac{\Omega_0}{2\Delta_0} \right)^2 R(\rho_j) \sum_{m \neq j} R(\rho_m) \left\{ (\hat{\mathbf{z}} - \hat{\mathbf{r}}_{jm}) \frac{\sin[k_0(r_{jm} - z_{jm}) - \ell\phi_{jm}]}{k_0 r_{jm}} - \hat{\mathbf{r}}_{jm} \frac{\cos[k_0(r_{jm} - z_{jm}) - \ell\phi_{jm}]}{(k_0 r_{jm})^2} \right\} \\ &+ \hbar \Gamma \left(\frac{\Omega_0}{2\Delta_0} \right)^2 R(\rho_j) \left[\frac{\ell}{\rho_j} - \frac{2\rho_j}{w^2} \right] \sum_{m \neq j} R(\rho_m) \frac{\cos[k_0(r_{jm} - z_{jm}) - \ell\phi_{jm}]}{k_0 r_{jm}} \hat{\mathbf{u}}_\rho \\ &+ \ell \hbar \Gamma \left(\frac{\Omega_0}{2\Delta_0} \right)^2 \frac{R(\rho_j)}{\rho_j} \sum_{m \neq j} R(\rho_m) \frac{\sin[k_0(r_{jm} - z_{jm}) - \ell\phi_{jm}]}{k_0 r_{jm}} \hat{\mathbf{u}}_\phi + \mathbf{F}_{Lj}, \end{aligned} \quad (19)$$

where $\phi_{jm} = \phi_j - \phi_m$, $r_{jm} = |\mathbf{r}_j - \mathbf{r}_m|$, and $\hat{\mathbf{r}}_{jm} = (\mathbf{r}_j - \mathbf{r}_m)/r_{jm}$, which is the unit vector along the distance between \mathbf{r}_j and \mathbf{r}_m . The first term of the right-hand side of Eq. (19) is

$$\times \sum_{\mathbf{k}} a_{\mathbf{k}} e^{-i(\mathbf{k}_0 - \mathbf{k}) \cdot \mathbf{r}_j - i\delta_k t} + \text{H.c.} \left. \right\} + \mathbf{F}_{Lj}, \quad (15)$$

$$\dot{a}_{\mathbf{k}} = -ig \sum_{j=1}^N R(\rho_j) e^{i(\mathbf{k}_0 - \mathbf{k}) \cdot \mathbf{r}_j + i\ell\phi_j + i\delta_k t}, \quad (16)$$

where $j = 1, \dots, N$, $\delta_k = \omega_k - \omega_0$, $g = g_k(\Omega_0/2\Delta_0)$, and the sum in \mathbf{k} is over all the vacuum three-dimensional modes. In the right-hand side of Eq. (15), the first term is the force proportional to the photon momentum exchange $\hbar(\mathbf{k}_0 - \mathbf{k})$ [13], whereas the second term is the collective force proportional to the gradient of the pump amplitude profile and of the azimuthal phase. In the limit $\Delta_0 \gg \Gamma$ the single-atom force (10) takes the form

$$\begin{aligned} \mathbf{F}_{Lj} &= \Gamma \left[\frac{\Omega_0 R(\rho_j)}{2\Delta_0} \right]^2 \left(\hbar k_0 \hat{\mathbf{u}}_z + \frac{\hbar \ell}{\rho_j} \hat{\mathbf{u}}_\phi \right) \\ &+ \frac{\hbar [\Omega_0 R(\rho_j)]^2}{2\Delta_0} \left[\frac{\ell}{\rho_j} - \frac{2\rho_j}{w^2} \right] \hat{\mathbf{u}}_\rho. \end{aligned} \quad (17)$$

Equations (14)–(16) extend the single-mode OAM-CARL described in [9], where the atoms are assumed to scatter the pump photons in a copropagating, with $\mathbf{k} = \mathbf{k}_0$, and counterrotating Laguerre-Gaussian mode $\text{LG}_{0-\ell}$ with the same beam waist w . Furthermore, [9] assumes the atoms trapped in a thin circular ring in the transverse plane such that the radial motion is negligible, i.e., ρ_j is constant and equal to $\rho = w\sqrt{\ell/2}$ [for which $R(\rho)$ is maximum]. In this case the evolution of the atomic cloud is essentially one-dimensional, in the azimuthal coordinate alone.

E. Superradiant OAM-CARL model

In free space we can assume the Markov approximation and adiabatically eliminate the multimode radiation field $a_{\mathbf{k}}$ in Eqs. (14)–(16) (see Appendix B). The resulting equations are

due to the collective momentum recoil, weighted by the radial profile $R(\rho)$ of the pump field; the second term is a collective radial force, due to variation of the radial profile of the pump;

and the third one is the collective azimuth force, proportional to the gradient of the OAM pump phase. It is possible to return to the results obtained for CARL in free space in [13], where the atoms are driven by a plane wave, by considering the first term only, with $R(\rho_j) = 1$ and $\ell = 0$. We outline that the model described by Eqs. (18) and (19) assumes classical atomic motion, considering the atoms as point particles with well-defined position and momentum. Generally, this condition is realized when the superradiant scattering rate is larger than the recoil frequency [18]. Furthermore, we neglect the thermal motion, assuming the temperature low enough such that we can neglect the Doppler broadening induced by the thermal velocities.

F. Scattered field

The scattered intensity in the far-field limit, for $\mathbf{r} \gg \mathbf{r}_j$, is

$$I_s(\mathbf{k}) = I_1 N^2 |M(\mathbf{k}, t)|^2, \quad (20)$$

where $I_1 = (\hbar\omega_0\Gamma/8\pi r^2)(\Omega_0/2\Delta_0)^2$ is the single-atom Rayleigh scattering intensity and

$$M(\mathbf{k}, t) = \frac{1}{N} \sum_{j=1}^N R(\rho_j) e^{i(\mathbf{k}_0 - \mathbf{k}) \cdot \mathbf{r}_j(t) + i\ell\phi_j(t)} \quad (21)$$

is the ‘‘optical magnetization,’’ or ‘‘bunching factor.’’ The direction of the scattered field is determined by the wave vector \mathbf{k} in Eq. (21), which depends on the spatial distribution of the atoms.

III. ATOMS IN A TRANSVERSE PLANE

We are interested in the case where the atoms are confined in the transverse plane, with $z_j = 0$. Then Eq. (19) becomes

$$\begin{aligned} \dot{\mathbf{p}}_j = & -\Gamma \hbar k_0 \left(\frac{\Omega_0}{2\Delta_0} \right)^2 R(\rho_j) \sum_{m \neq j} R(\rho_m) \left\{ \frac{\sin[k_0 \rho_{jm} - \ell \phi_{jm}]}{k_0 \rho_{jm}} + \frac{\cos[k_0 \rho_{jm} - \ell \phi_{jm}]}{(k_0 \rho_{jm})^2} \right\} \hat{\mathbf{u}}_{jm} + \hbar \Gamma \left(\frac{\Omega_0}{2\Delta_0} \right)^2 R(\rho_j) \\ & \times \left[\frac{|\ell|}{\rho_j} - \frac{2\rho_j}{w^2} \right] \sum_{m \neq j} R(\rho_m) \frac{\cos[k_0 \rho_{jm} - \ell \phi_{jm}]}{k_0 \rho_{jm}} \hat{\mathbf{u}}_\rho + \ell \hbar \Gamma \left(\frac{\Omega_0}{2\Delta_0} \right)^2 \frac{R(\rho_j)}{\rho_j} \sum_{m=1}^N R(\rho_m) \frac{\sin[k_0 \rho_{jm} - \ell \phi_{jm}]}{k_0 \rho_{jm}} \hat{\mathbf{u}}_\phi + \mathbf{F}_{\rho_j}, \end{aligned} \quad (22)$$

where $\hat{\mathbf{u}}_{jm} = (\mathbf{r}_{\perp j} - \mathbf{r}_{\perp m})/\rho_{jm}$, with $\rho_{jm} = \sqrt{\rho_j^2 + \rho_m^2 - 2\rho_j \rho_m \cos \phi_{jm}}$ and $\mathbf{r}_{\perp j} = \rho_j \cos \phi_j \hat{\mathbf{u}}_x + \rho_j \sin \phi_j \hat{\mathbf{u}}_y$. The last term in Eq. (22) is the single-atom radial force exerted by the pump:

$$\mathbf{F}_{\rho_j} = \frac{\hbar[\Omega_0 R(\rho_j)]^2}{2\Delta_0} \left(\frac{\ell}{\rho_j} - \frac{2\rho_j}{w^2} \right) \hat{\mathbf{u}}_\rho. \quad (23)$$

We have neglected the longitudinal radiation pressure force \mathbf{F}_{z_j} and included the azimuthal force \mathbf{F}_{ϕ_j} in the last sum over m of Eq. (22), with the term $m = j$. This is a rather surprising result which will have important consequences in the occurrence of the azimuthal CARL instability, and it will be discussed in Sec. V.

By projecting Eq. (22) along the radial and azimuthal directions, we obtain

$$\ddot{\rho}_j = \sum_{m \neq j} \frac{f_{jm}}{\rho_{jm}} (\rho_j - \rho_m \cos \phi_{jm}) + h_j + \rho_j \dot{\phi}_j^2, \quad (24)$$

$$2\dot{\rho}_j \dot{\phi}_j + \rho_j \ddot{\phi}_j = \sum_{m \neq j} \frac{f_{jm}}{\rho_{jm}} \rho_m \sin \phi_{jm} + g_j, \quad (25)$$

with

$$f_{jm} = -\Gamma \frac{\hbar k_0}{M} \left(\frac{\Omega_0}{2\Delta_0} \right)^2 R(\rho_j) R(\rho_m) \left\{ \frac{\sin(k_0 \rho_{jm} - \ell \phi_{jm})}{k_0 \rho_{jm}} + \frac{\cos(k_0 \rho_{jm} - \ell \phi_{jm})}{(k_0 \rho_{jm})^2} \right\}, \quad (26)$$

$$h_j = \frac{\hbar \Gamma}{M} \left(\frac{\Omega_0}{2\Delta_0} \right)^2 R(\rho_j) \left[\frac{\ell}{\rho_j} - \frac{2\rho_j}{w^2} \right] \left\{ \sum_{m \neq j} R(\rho_m) \frac{\cos(k_0 \rho_{jm} - \ell \phi_{jm})}{k_0 \rho_{jm}} + \frac{2\Delta_0}{\Gamma} R(\rho_j) \right\}, \quad (27)$$

$$g_j = \ell \frac{\hbar \Gamma}{M} \left(\frac{\Omega_0}{2\Delta_0} \right)^2 \frac{R(\rho_j)}{\rho_j} \sum_{m=1}^N R(\rho_m) \frac{\sin(k_0 \rho_{jm} - \ell \phi_{jm})}{k_0 \rho_{jm}}. \quad (28)$$

We observe that the first term on the right-hand side of Eq. (22) gives both a radial and azimuthal contribution to the force [term f_{jm} in Eqs. (24) and (25)], whereas its second term and the pump gradient force \mathbf{F}_{ρ_j} give a purely radial force [term h_j in Eq. (24)]. Finally the third term of the right-hand side of Eq. (22) gives an azimuthal force proportional to the index ℓ [term g_j in Eq. (25)].

Considering the emission only in the transverse plane, with $\mathbf{k} = k_0 \cos \theta \hat{\mathbf{u}}_x + k_0 \sin \theta \hat{\mathbf{u}}_y$, the optical magnetization becomes

$$M(\theta) = \frac{1}{N} \sum_{j=1}^N R(\rho_j) e^{-ik_0 \rho_j \cos(\theta - \phi_j) + i\ell \phi_j}. \quad (29)$$

We observe that its phase is modulated by the different atomic positions in the transverse plane. Using the identity

$$e^{iz \cos \phi} = \sum_{m=-\infty}^{+\infty} i^m J_m(z) e^{im\phi}, \quad (30)$$

where $J_m(z)$ is the m th-order Bessel function, we can write

$$M(\theta) = \sum_{m=-\infty}^{+\infty} P_{\ell,m} e^{im\theta}, \quad (31)$$

$$\begin{aligned} \ddot{\phi}_j = \omega_r \Gamma \left(\frac{\Omega_0}{2\Delta_0} \right)^2 \frac{R^2(\rho)}{(k_0 \rho)^2} \left\{ - \sum_{m \neq j} \cot(\phi_{jm}/2) \left[\sin[2k_0 \rho |\sin(\phi_{jm}/2)| - \ell \phi_{jm}] + \frac{\cos[2k_0 \rho |\sin(\phi_{jm}/2)| - \ell \phi_{jm}]}{2k_0 \rho |\sin(\phi_{jm}/2)|} \right] \right. \\ \left. + \ell \sum_{m=1}^N \frac{\sin[2k_0 \rho |\sin(\phi_{jm}/2)| - \ell \phi_{jm}]}{k_0 \rho |\sin(\phi_{jm}/2)|} \right\}. \end{aligned} \quad (33)$$

We observe that, if $\rho = w/\sqrt{2} = 1/k_\theta$, the torque on the j atom is proportional to the angular recoil frequency $\omega_\theta = \hbar k_\theta^2 / 2M$ rather than to the recoil frequency ω_r . When ρ_j is constant the optical magnetization can be written as

$$\begin{aligned} M(\theta) &= \frac{R(\rho)}{N} \sum_{j=1}^N e^{-ik_0 \rho \cos(\theta - \phi_j) + i\ell \phi_j} \\ &= R(\rho) \sum_m (-i)^m J_m(k_0 \rho) \Phi_{m-\ell} e^{im\theta}, \end{aligned} \quad (34)$$

where

$$\Phi_n = \frac{1}{N} \sum_{j=1}^N e^{-in\phi_j} \quad (35)$$

is the azimuthal bunching on the n th harmonic. In the case of a uniform distribution of the phases ϕ_j , its expression becomes

$$M(\theta) = R(\rho) (-i)^\ell J_\ell(k_0 \rho) e^{i\ell\theta}, \quad (36)$$

so that $|M(\theta)| = R(\rho) |J_\ell(k_0 \rho)|$ and the scattered intensity is isotropic in the transverse plane. This is true also if the phases are perfectly bunched around a single value, $\phi_j = \phi_0$:

$$M(\theta) = R(\rho) e^{i\ell\phi_0 - i\rho \cos(\theta - \phi_0)}, \quad (37)$$

with $|M(\theta)| = R(\rho)$. More generally, $M(\theta)$ is a superposition of different harmonics.

V. AZIMUTHAL OAM-CARL MODEL

We study the azimuthal motion of the atoms in the two-dimensional transverse plane, described by Eqs. (33). To avoid

where

$$P_{\ell,m} = (-i)^m \frac{1}{N} \sum_{j=1}^N R(\rho_j) J_m(k_0 \rho_j) e^{i(\ell-m)\phi_j}. \quad (32)$$

Hence, the angular distribution of the scattered intensity is determined by the radial and azimuthal atomic positions.

IV. ATOMS ON A RING

Let us consider the case where the atoms are trapped in a thin circular ring in the transverse plane such that the radial motion of the atoms is negligible, i.e., $\rho_j = \rho$ is constant. Then, the evolution of the atomic motion is essentially one-dimensional in the azimuthal angle ϕ_j . By considering $\rho_{jm} = 2\rho |\sin(\phi_{jm}/2)|$, together with Eqs. (24) and (25), we obtain the azimuthal equation

the singularity for $\phi_{jm} \rightarrow 0$, we introduce a cutoff ϵ such that

$$|\sin(\phi_{jm}/2)| \rightarrow \sqrt{\sin^2(\phi_{jm}/2) + \epsilon^2} \equiv q_{jm}. \quad (38)$$

Furthermore, since ρ is kept constant, we rescale the time t into the dimensionless time $t' = \beta t$, with

$$\beta = \sqrt{\omega_r \Gamma} \left(\frac{\Omega_0}{2\Delta_0} \frac{R(\rho)}{k_0 \rho} \right). \quad (39)$$

Hence, the working equations are

$$\begin{aligned} \frac{d^2 \phi_j}{dt'^2} &= - \sum_{m \neq j} \frac{\sin(\phi_{jm})}{2q_{jm}^2} \\ &\times \left\{ \sin[2k_0 \rho q_{jm} - \ell \phi_{jm}] + \frac{\cos[2k_0 \rho q_{jm} - \ell \phi_{jm}]}{2k_0 \rho q_{jm}} \right\} \\ &+ \ell \sum_{m=1}^N \frac{\sin[2k_0 \rho q_{jm} - \ell \phi_{jm}]}{k_0 \rho q_{jm}}. \end{aligned} \quad (40)$$

For a single atom, in the limit $\epsilon \rightarrow 0$ the unscaled equation for the single atom with phase ϕ is

$$\ddot{\phi} = 2\ell \beta^2 = \ell \frac{\hbar \Gamma}{M \rho^2} \left(\frac{\Omega_0 R(\rho)}{2\Delta_0} \right)^2. \quad (41)$$

It can be written in terms of the atomic angular momentum along the z axis, $L_z = M \rho^2 \dot{\phi}$:

$$\dot{L}_z = \ell \hbar \Gamma \left(\frac{\Omega_0 R(\rho)}{2\Delta_0} \right)^2 = T_z, \quad (42)$$

where T_z is the torque exerted by the OAM pump, in agreement with [7]. In the scattering force, the pump photon also transfers, other than its linear momentum $\hbar \mathbf{k}_0$, its angular

momentum $(\hbar\ell)\hat{\mathbf{z}}$, and the torque T_z is equal to the photon angular momentum $\hbar\ell$ times the scattering rate.

Let us write Eq. (40) in the form

$$\frac{d^2\phi_j}{dt^2} = \sum_{m=1}^N G(\phi_j - \phi_m) \quad (43)$$

with $j = 1, \dots, N$ and where

$$G(x) = -\frac{\sin x}{2q(x)^2} \left[\sin[2\rho'q(x) - \ell x] + \frac{\cos[2\rho'q(x) - \ell x]}{2\rho'q(x)} \right] + \ell \frac{\sin[2\rho'q(x) - \ell x]}{\rho'q(x)}, \quad (44)$$

$\rho' = k_0\rho$, and

$$q(x) = \sqrt{\sin^2(x/2) + \epsilon^2}. \quad (45)$$

An important feature is that the force $G(\phi_j - \phi_m)$ on particle j due to particle m does not have the symmetry of a force derivable from a two-body interaction potential, which is a function solely of the separation between particles, i.e., $G(\phi_j - \phi_m) \neq -G(\phi_m - \phi_j)$. As a consequence, the average angular velocity $\langle \dot{\phi} \rangle = (1/N) \sum_{j=1}^N \dot{\phi}_j$ is not conserved in time. The dynamics of Eqs. (43) are not derivable from an underlying Hamiltonian, so that one may not associate an energy function with the system [19].

The function $G(x)$ can be derived from a potential $V(x)$:

$$G(x) = -\frac{d}{dx}V(x), \quad (46)$$

where

$$V(x) = -\frac{\cos[2\rho'q(x) - \ell x]}{\rho'q(x)}. \quad (47)$$

Therefore, Eq. (43) can be rewritten as

$$\frac{d^2\phi_j}{dt^2} = -\frac{\partial}{\partial\phi_j} \sum_{m=1}^N V(\phi_j - \phi_m). \quad (48)$$

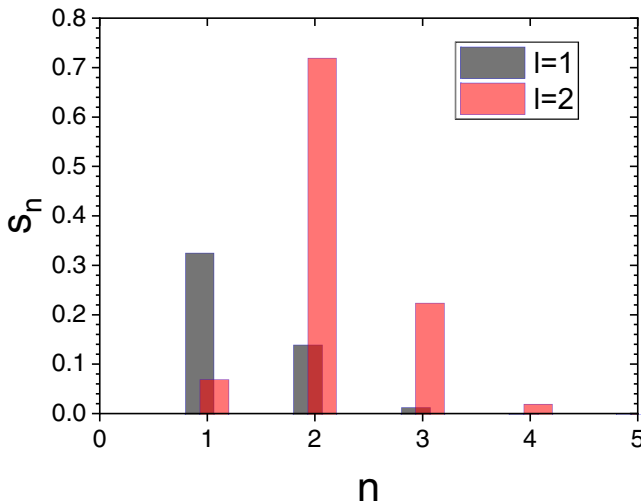


FIG. 2. s_n vs n for $\ell = 1$ and 2 , $k_0\rho = 1$, and $\epsilon = 0.1$.

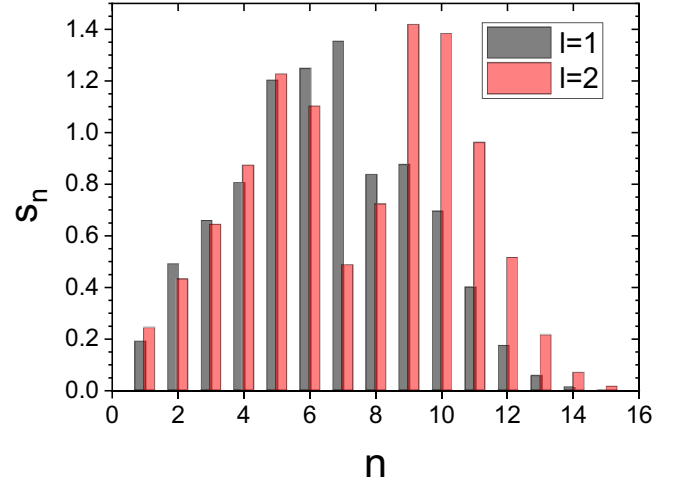


FIG. 3. s_n vs n for $\ell = 1$ and 2 , $k_0\rho = 10$, and $\epsilon = 0.1$.

A. Equilibrium

In the case the phases are uniformly distributed (no bunching), we consider ϕ_j as continuous variables ϕ and we approximate the sum in Eq. (48) by an integral:

$$\begin{aligned} \frac{d^2\phi}{dt^2} &= -\frac{N}{2\pi} \frac{\partial}{\partial\phi} \int_0^{2\pi} d\phi' V(\phi - \phi') \\ &= \frac{N}{2\pi} \int_0^{2\pi} d\phi' \frac{\partial V(\phi - \phi')}{\partial\phi'}. \end{aligned} \quad (49)$$

Changing the integration variable into $x = \phi - \phi'$ and using the fact that $V(x)$ is periodic between zero and 2π , we can write

$$\begin{aligned} \frac{d^2\phi}{dt^2} &= -\frac{N}{2\pi} \int_{\phi}^{\phi+2\pi} dx \frac{dV(x)}{dx} \\ &= -\frac{N}{2\pi} [V(\phi + 2\pi) - V(\phi)] = 0. \end{aligned} \quad (50)$$

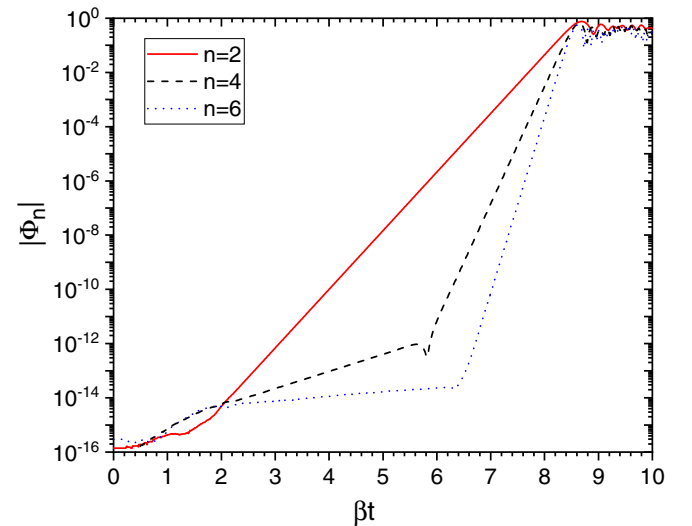


FIG. 4. Bunching $|\Phi_n|$ vs time βt , for $k_0\rho = 1$ and $\ell = 1$. The other parameters of the simulation are $N = 100$ and $\epsilon = 1$.

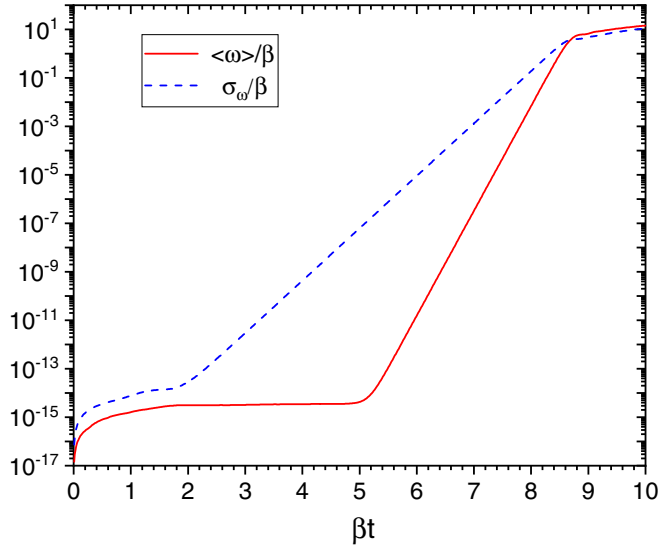


FIG. 5. Average angular velocity $\langle \omega \rangle / \beta$ and spread $\sigma_\omega / \beta = \sqrt{\langle \omega^2 \rangle - \langle \omega \rangle^2} / \beta$ vs time βt , for $k_0 \rho = 1$ and $\ell = 1$.

Hence, if the distribution of the phases is uniform, the force on every atom is zero and the system is in equilibrium. The system is unstable under small perturbations of this initial conditions, with a rate proportional to \sqrt{N} and a lethargy time proportional to $\ln(N)$, as it will be proved in the next section.

B. Stability analysis

We have proved that the azimuthal motion equation Eq. (43) has an equilibrium for $\phi_j = \phi_j^{(0)}$, such that

$$\sum_m G(\phi_j^{(0)} - \phi_m^{(0)}) = 0 \quad (51)$$

and $\dot{\phi}_j = 0$. Let us perturb the equilibrium, $\phi_j(t) = \phi_j^{(0)} + \delta\phi_j(t)$, with $\delta\phi_j \ll \phi_j^{(0)}$. Then, the linearized n th harmonic

azimuthal bunching

$$\delta\Phi_n(t') = \frac{1}{N} \sum_j e^{-in\phi_j^{(0)}} \delta\phi_j(t') \quad (52)$$

grows in time as $\Phi_n(t') \propto e^{\lambda_n t'}$ (see Appendix C), where

$$\lambda_n = \pm in\sqrt{NV_n}, \quad (53)$$

and where V_n is the Fourier transform of the potential $V(x)$:

$$V_n = \frac{1}{2\pi} \int_0^{2\pi} V(x) e^{-inx} dx. \quad (54)$$

Hence, the azimuthal superradiant rate for the n th harmonic bunching is

$$\Gamma_n = \sqrt{N}\beta s_n(k_0\rho, \ell) = \sqrt{\omega_r \Gamma N} \left(\frac{\Omega_0}{2\Delta_0} \frac{R(\rho)}{k_0\rho} \right) s_n, \quad (55)$$

where

$$s_n = n |\text{Im}\sqrt{V_n}|. \quad (56)$$

The corresponding frequency shift is

$$\delta\Omega_n = \sqrt{N}\beta\delta\omega_n = \sqrt{\omega_r \Gamma N} \left(\frac{\Omega_0}{2\Delta_0} \frac{R(\rho)}{k_0\rho} \right) \delta\omega_n, \quad (57)$$

with

$$\delta\omega_n = n \text{Re}\sqrt{V_n}. \quad (58)$$

We observe that the superradiant rate scales as \sqrt{N} , typical for superradiance in a classical system [18]. Figure 2 shows s_n as a function of n for $k_0\rho = 1$, $\ell = 1$, and $\ell = 2$. The cutoff is set to $\epsilon = 0.1$. We observe that for a very focused beam ($k_0\rho \leq 1$) the maximum bunching occurs for the harmonic $n = \ell$. However, things become more complex when the ring radius is larger, for $k_0\rho \gg 1$. Figure 3 shows s_n as a function of n for $k_0\rho = 10$, with $\ell = 1$ and 2: In these cases the harmonic distribution is wider, with a single maximum around $n = 7$ for $\ell = 1$ and two relative maxima around $n = 5$ and 10 for $\ell = 2$. Finally, the condition in order to neglect quantum effects in the atomic motion is that the superradiant rate $\sqrt{N}\beta$ must be larger than the azimuthal recoil frequency $\omega_\phi = \hbar/2M\rho^2 = \omega_r/(k_0\rho)^2$.

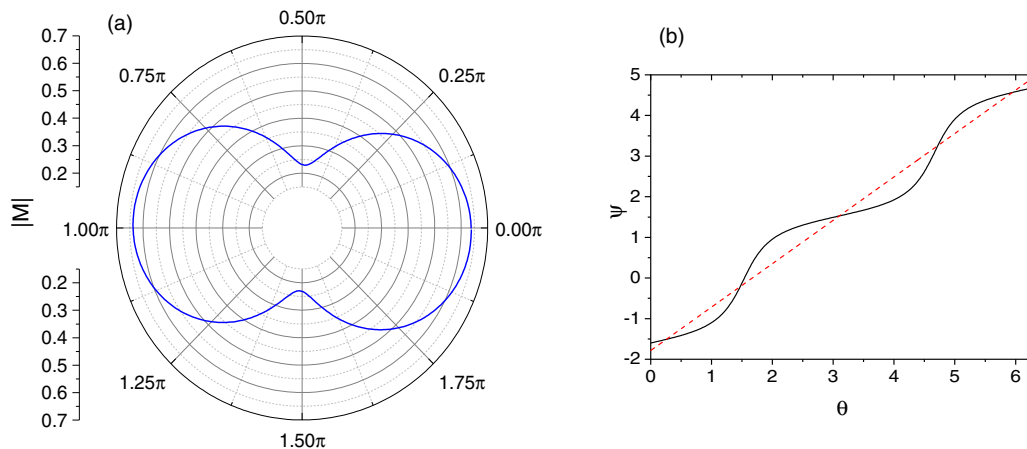
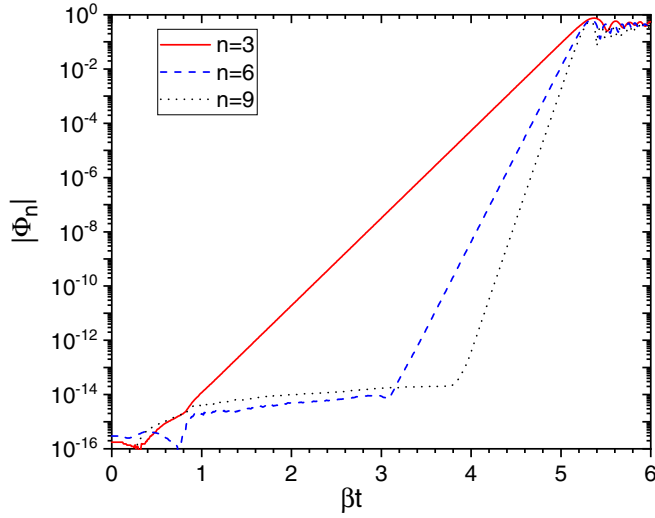


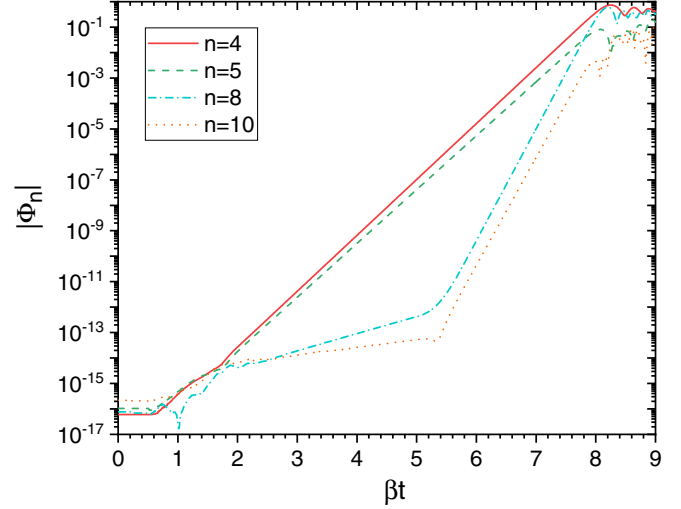
FIG. 6. Optical magnetization $M(\theta) = |M(\theta)| \exp(i\psi)$ for $k_0\rho = 1$ and $\ell = 1$, at $\beta t = 8.5$. (a) Polar plot of $|M(\theta)|$. (b) Phase ψ vs θ . The dashed line is a linear fit with $\psi = -1.78 + 1.06\theta$.


 FIG. 7. Bunching $|\Phi_n|$ vs time βt , for $k_0\rho = 1$ and $\ell = 2$.

VI. NUMERICAL RESULTS

Equation (40) has been solved numerically for different values of ρ and ℓ . The parameters assumed have been $N = 100$ and $\epsilon = 1$, in order to avoid numerical instabilities occurring when two particles become too close to each other. In a real system, with many atoms distributed in larger volumes, this issue should be less critical, with few particles kicked off by pair collisions. The results presented here, in an idealized situation in which the atoms have negligible thermal motion and are distributed on a ring of zero thickness, have the objective to show the typical features of the collective effects observable by a laser beam possessing an OAM beam incident on the atoms confined in a transverse annular volume. An extension of the analysis including also the radial dynamics and the temperature effects will be presented elsewhere.

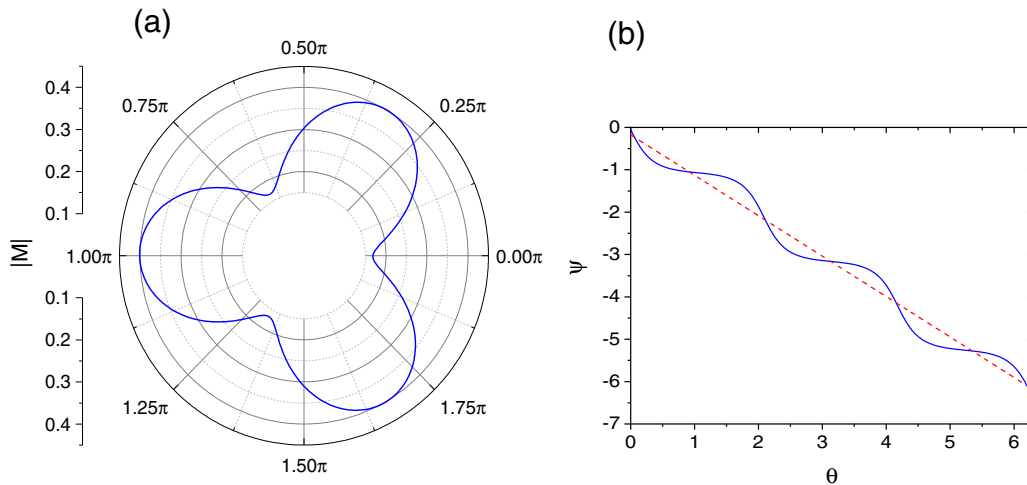
First, we have considered a case of a tightly focused laser beam, with $k_0\rho = 1$. Figure 4 shows the azimuthal bunching $|\Phi_n|$ vs time for $\ell = 1$. The growth occurs for $n = 2$ and its


 FIG. 9. Bunching $|\Phi_n|$ vs time βt , for $k_0\rho = 10$ and $\ell = 1$.

first harmonics $n = 4, 6$, up to a value close to unity, corresponding to the atoms bunched around two opposite phases, with difference π . The atoms start to rotate counterclockwise when the bunching $|\Phi_2|$ becomes significant, as can be seen in Fig. 5, showing the average angular velocity $\langle\omega\rangle/\beta$ vs time (where $\omega_j = d\phi_j/dt$) (full red line) and the spread of the angular velocity $\sigma_\omega/\beta = \sqrt{\langle\omega^2\rangle - \langle\omega\rangle^2}/\beta$. The phases are accelerated up to an angular velocity of about 10β . Figure 6 shows the polar plot of $|M(\theta)|$ [Fig. 6(a)] and its phase ψ [Fig. 6(b)] vs θ , where $M(\theta) = |M(\theta)| \exp[i\psi(\theta)]$. The emission occurs in the transverse plane within two lobes, in a typical bipolar distribution, rotating with the atomic average angular velocity. We observe that the scattered field is, from Eq. (34),

$$M(\theta) \sim R(\rho)e^{i\theta} \{J_1(k_0\rho)[1 - i\Phi_2^*e^{-2i\theta}] - J_3(k_0\rho)\Phi_2e^{2i\theta}\}. \quad (59)$$

Since $J_3(k_0\rho) \ll J_1(k_0\rho)$ and $|\Phi_2| < 1$, the phase is $\psi(\theta) \sim \theta_0 + \theta$ with a modulation $\propto \sin(2\theta + \theta_{02})$ [see Fig. 6(b)]. A


 FIG. 8. Optical magnetization $M(\theta) = |M(\theta)| \exp(i\psi)$ for $k_0\rho = 1$ and $\ell = 2$, at $\beta t = 8.5$. (a) Polar plot of $|M(\theta)|$. (b) Phase ψ vs θ . The dashed line is a linear fit with $\psi = -0.17 - 0.95\theta$.

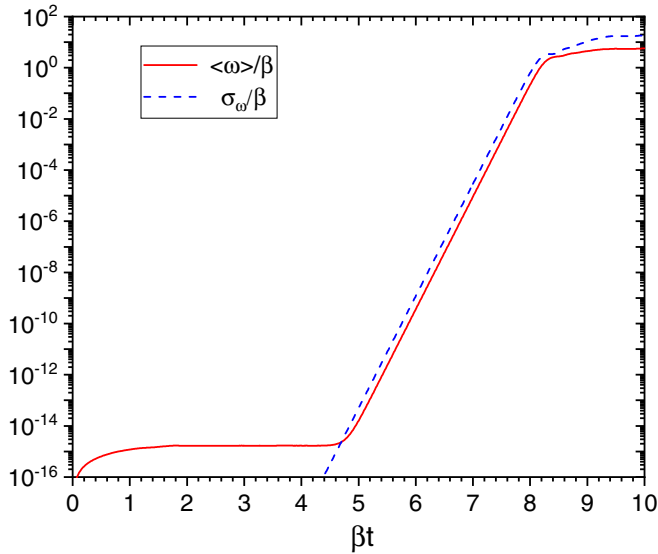


FIG. 10. Average angular velocity $\langle \omega \rangle / \beta$ and spread $\sigma_\omega / \beta = \sqrt{\langle \omega^2 \rangle - \langle \omega \rangle^2} / \beta$ vs time βt , for $k_0 \rho = 10$ and $\ell = 1$.

similar behavior is observed for $k_0 \rho = 1$ and $\ell = 2$, in Figs. 7 and 8: Now the angular bunching is for $n = 3$ and for its harmonics [see Fig. 7], whereas the field angular distribution has three symmetric lobes [see Fig. 8(a)], meaning that the atoms bunch around three phases separated by $2\pi/3$. The field in this case is

$$M(\theta) \sim iR(\rho)e^{-i\theta}[J_1(k_0\rho)\Phi_3^* + iJ_2(k_0\rho)e^{3i\theta} - J_5(k_0\rho)\Phi_3e^{6i\theta}]. \quad (60)$$

Since $J_5(k_0\rho) \ll J_2(k_0\rho) \ll J_1(k_0\rho)$ and $|\Phi_3| < 1$, the phase is now $\psi(\theta) \sim \theta_0 - \theta$ with a modulation as $\sin(3\theta + \theta_{03})$ [see Fig. 8(b)].

Secondly, we consider a ring with a large radius, $k_0 \rho = 10$ in the example shown in Figs. 9–11. In this case more than one mode is exponentially amplified (see for instance the result of the linear analysis, Fig. 3). Figure 9, for $\ell = 1$, shows that two modes, $n = 4$ and 5 with their harmonics, are amplified, with a maximum value larger for the mode $n = 4$. Also in this case the atoms are set in rotation with a maximum average angular

velocity of $\langle \omega \rangle \sim 10\beta$ (see Fig. 10). The angular distribution and the phase of the field present a richer structure, as can be seen from Fig. 11. In particular, we observe the presence of four main lobes [see Fig. 11(a)] with a more complex secondary structure. In general, we observe that by increasing the ring radius we excite more and more modes. In the limit of large radius we expect that the emission distribution will tend to be isotropic in the transverse plane.

VII. CONCLUSIONS

We have presented a study of superradiant scattering of an optical field possessing OAM by a cold atomic gas using a multimode classical model in which no initial assumption about the spatial structure of the scattered field is made. For simplicity we restricted the analysis to the case where the atoms are distributed in a thin ring and the atomic dynamics involve azimuthal motion only. It was shown that a uniform angular distribution of atoms throughout the ring becomes unstable when illuminated with a far-detuned optical pump field, and that the instability is superradiant in character, resulting in spontaneous rotation of the gas and formation of atomic bunches around the ring and scattered light the phase profile of which is dependent on the pump OAM index, ℓ . A natural extension to the paper presented here is a relaxation of some of the assumptions used, e.g., the restriction to solely azimuthal dynamics to include also radial and even longitudinal dynamics to describe more complex spatial structures, and the extension to include polarization effects, as was done for CARL in [14]. This would allow study of interactions involving exchange of both OAM and SAM. Additionally, extension from cold, thermal gases to quantum degenerate gases opens up possibilities for new methods for creation of vortices and persistent currents in BECs, in addition to those described in [11,12].

ACKNOWLEDGMENTS

This work was performed in the framework of the European Training Network CoOpt, which is funded by the European Union (EU) Horizon 2020 program under the Marie Skłodowska-Curie action, Grant Agreement No. 721465.

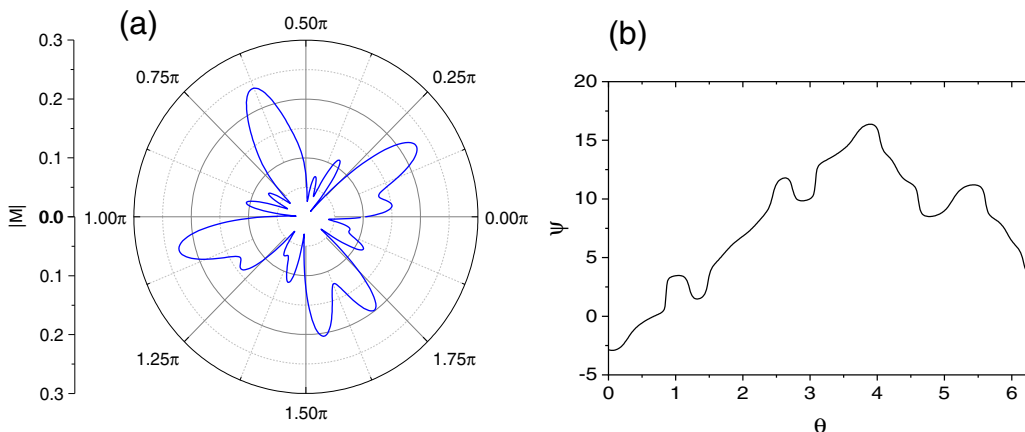


FIG. 11. Optical magnetization $M(\theta) = |M(\theta)| \exp(i\psi)$ for $k_0 \rho = 10$ and $\ell = 1$, at $\beta t = 8$. (a) Polar plot of $|M(\theta)|$. (b) Phase ψ vs θ .

APPENDIX A: DERIVATION OF THE MULTIMODE EQS. (14)–(16)

The force acting on the j th atom is obtained from the Heisenberg equation:

$$\dot{\mathbf{p}}_j = \frac{1}{i\hbar}[\mathbf{p}_j, H_L + H_V] = \mathbf{F}_j, \quad (\text{A1})$$

where H_L and H_V are given by Eqs. (5) and (6). Using cylindrical coordinates, the force \mathbf{F}_j is

$$\dot{\mathbf{F}}_j = \frac{\hbar\Omega_0}{2} \left\{ \sigma_j \left[ik_0 R(\rho_j) \hat{\mathbf{u}}_z - \frac{dR(\rho_j)}{d\rho_j} \hat{\mathbf{u}}_\rho + i\ell \frac{R(\rho_j)}{\rho_j} \hat{\mathbf{u}}_\phi \right] e^{-ik_0 z_j - i\ell\phi_j} - \text{H.c.} \right\} + i\hbar \left\{ \sigma_j \sum_{\mathbf{k}} \mathbf{k} g_{\mathbf{k}} a_{\mathbf{k}}^\dagger e^{i\delta_{\mathbf{k}} t - i\mathbf{k}\cdot\mathbf{r}_j} - \text{H.c.} \right\}, \quad (\text{A2})$$

with $\delta_{\mathbf{k}} = \omega_{\mathbf{k}} - \omega_0$. The Heisenberg equation for the multimode field operator $a_{\mathbf{k}}$ is

$$\dot{a}_{\mathbf{k}} = \frac{1}{i\hbar}[a_{\mathbf{k}}, H_V] = -ig_{\mathbf{k}} e^{i\delta_{\mathbf{k}} t} \sum_{j=1}^N \sigma_j e^{-i\mathbf{k}\cdot\mathbf{r}_j}. \quad (\text{A3})$$

By inserting the expression of σ_j , Eq. (9), in Eq. (A3), assuming $\Delta_0 \gg \Gamma$, and neglecting the vacuum field-induced term in Eq. (9), we obtain

$$\dot{a}_{\mathbf{k}} = -ig e^{i\delta_{\mathbf{k}} t} \sum_{j=1}^N R(\rho_j) e^{i(\mathbf{k}_0 - \mathbf{k})\cdot\mathbf{r}_j + i\ell\phi_j}, \quad (\text{A4})$$

with $g = g_{\mathbf{k}}(\Omega_0/2\Delta_0)$. To obtain the force on the j th atom, we insert Eq. (9) in Eq. (A2), assuming $\Delta_0 \gg \Gamma$ and neglecting the terms quadratic in the vacuum field $a_{\mathbf{k}}$. A straightforward calculation yields

$$\begin{aligned} \mathbf{F}_j = & i\hbar g R(\rho_j) \sum_{\mathbf{k}} (\mathbf{k}_0 - \mathbf{k}) \{ a_{\mathbf{k}} e^{-i(\mathbf{k}_0 - \mathbf{k})\cdot\mathbf{r}_j - i\ell\phi_j - i\delta_{\mathbf{k}} t} - \text{H.c.} \} \\ & - \hbar g \left\{ \left[\frac{dR(\rho_j)}{d\rho_j} \hat{\mathbf{u}}_\rho - i\ell \frac{R(\rho_j)}{\rho_j} \hat{\mathbf{u}}_\phi \right] \sum_{\mathbf{k}} a_{\mathbf{k}} e^{-i(\mathbf{k}_0 - \mathbf{k})\cdot\mathbf{r}_j - i\delta_{\mathbf{k}} t} + \text{H.c.} \right\} + \mathbf{F}_{Lj}, \end{aligned} \quad (\text{A5})$$

where \mathbf{F}_{Lj} is the force exerted by the laser beam, expressed by Eq. (17).

APPENDIX B: DERIVATION OF THE SUPERRADIANT EQS. (18) and (19)

In free space the light is scattered in the 3D vacuum modes. Following [13], we eliminate the scattered field by integrating Eq. (16) to obtain

$$a_{\mathbf{k}}(t) = a_{\mathbf{k}}(0) e^{-i(\omega_{\mathbf{k}} - \omega_0)t} - igN \int_0^t \rho_{\mathbf{k}_0 - \mathbf{k}}(t - \tau) e^{-i(\omega_{\mathbf{k}} - \omega_0)\tau} d\tau, \quad (\text{B1})$$

with

$$\rho_{\mathbf{q}}(t) = \frac{1}{N} \sum_{j=1}^N R(\rho_j) e^{i\ell\phi_j} e^{i\mathbf{q}\cdot\mathbf{r}_j(t)}. \quad (\text{B2})$$

The first term in Eq. (B1) gives the free electromagnetic field, i.e., vacuum fluctuations, and the second term is the radiation field due to Rayleigh scattering. If Eq. (B1) is substituted into Eq. (15) for \mathbf{p}_j , we obtain

$$\begin{aligned} \dot{\mathbf{p}}_j = & \hbar g^2 N \sum_{\mathbf{k}} (\mathbf{k}_0 - \mathbf{k}) \int_0^t d\tau R(\rho_j) [\rho_{\mathbf{k}_0 - \mathbf{k}}(t - \tau) e^{-i(\mathbf{k}_0 - \mathbf{k})\cdot\mathbf{r}_j - i\ell\phi_j} e^{-i(\omega_{\mathbf{k}} - \omega_0)\tau} + \text{H.c.}] + i\hbar g^2 N \sum_{\mathbf{k}} \int_0^t d\tau \\ & \times \left\{ \left[\frac{dR(\rho_j)}{d\rho_j} \hat{\mathbf{u}}_\rho - i\ell \frac{R(\rho_j)}{\rho_j} \hat{\mathbf{u}}_\phi \right] \rho_{\mathbf{k}_0 - \mathbf{k}}(t - \tau) e^{-i(\mathbf{k}_0 - \mathbf{k})\cdot\mathbf{r}_j} e^{-i(\omega_{\mathbf{k}} - \omega_0)\tau} + \text{H.c.} \right\} + \mathbf{F}_{Lj}, \end{aligned} \quad (\text{B3})$$

where the first term of Eq. (B1) has been neglected. Then, transforming the sum over \mathbf{k} into an integral and using Eq. (B2), we attain the following expression:

$$\begin{aligned} \dot{\mathbf{p}}_j = & \hbar g^2 \frac{V_{ph}}{8\pi^3} \sum_{m \neq j} R(\rho_j) R(\rho_m) \left[e^{-i\mathbf{k}_0 \cdot (\mathbf{r}_j - \mathbf{r}_m) - i\ell(\phi_j - \phi_m)} \int_0^t d\tau e^{i\omega_0\tau} \int d\mathbf{k} (\mathbf{k}_0 - \mathbf{k}) e^{i\mathbf{k} \cdot (\mathbf{r}_j - \mathbf{r}_m)} e^{-i\mathbf{k} \cdot \mathbf{r}_m} + \text{H.c.} \right] + i\hbar g^2 \frac{V_{ph}}{8\pi^3} \sum_{m \neq j} R(\rho_m) \\ & \times \left\{ \left[\frac{dR(\rho_j)}{d\rho_j} \hat{\mathbf{u}}_\rho - i\ell \frac{R(\rho_j)}{\rho_j} \hat{\mathbf{u}}_\phi \right] e^{-i\mathbf{k}_0 \cdot (\mathbf{r}_j - \mathbf{r}_m) - i\ell(\phi_j - \phi_m)} \int_0^t d\tau e^{i\omega_0\tau} \int d\mathbf{k} e^{i\mathbf{k} \cdot (\mathbf{r}_j - \mathbf{r}_m)} e^{-i\mathbf{k} \cdot \mathbf{r}_m} - \text{H.c.} \right\} + \mathbf{F}_{Lj}, \end{aligned} \quad (\text{B4})$$

in which we used the Markov approximation so that $\mathbf{r}_j(t - \tau) \approx \mathbf{r}_j(t)$. We use the results of [13] to write

$$\int d\mathbf{k} e^{i\mathbf{k}\cdot(\mathbf{r}_j-\mathbf{r}_m)} e^{-ick\tau} = \frac{4\pi^2 k_0^2}{c} \frac{1}{ik_0 r_{jm}} [\delta(\tau - r_{jm}/c) - \delta(\tau + r_{jm}/c)], \quad (\text{B5})$$

$$\int d\mathbf{k} \mathbf{k} e^{i\mathbf{k}\cdot(\mathbf{r}_j-\mathbf{r}_m)} e^{-ick\tau} = \frac{4\pi^2 k_0^3}{c} \left\{ \frac{1}{ik_0 r_{jm}} [\delta(\tau - r_{jm}/c) + \delta(\tau + r_{jm}/c)] + \frac{1}{(k_0 r_{jm})^2} [\delta(\tau - r_{jm}/c) - \delta(\tau + r_{jm}/c)] \right\} \hat{\mathbf{r}}_{jm}, \quad (\text{B6})$$

with $\mathbf{r}_{jm} = \mathbf{r}_j - \mathbf{r}_m$, $r_{jm} = |\mathbf{r}_{jm}|$, and $\hat{\mathbf{r}}_{jm} = \mathbf{r}_{jm}/r_{jm}$. By inserting these expressions into Eq. (B4), together with the definitions of g and Γ , it is straightforward to arrive to the following expression of the force equation:

$$\begin{aligned} \dot{\mathbf{p}}_j &= \Gamma \hbar k_0 \left(\frac{\Omega_0}{2\Delta_0} \right)^2 R(\rho_j) \sum_{m \neq j} R(\rho_m) \left\{ (\hat{\mathbf{z}} - \hat{\mathbf{r}}_{jm}) \frac{\sin[k_0(r_{jm} - z_{jm}) - \ell\phi_{jm}]}{k_0 r_{jm}} - \hat{\mathbf{r}}_{jm} \frac{\cos[k_0(r_{jm} - z_{jm}) - \ell\phi_{jm}]}{(k_0 r_{jm})^2} \right\} \\ &+ \hbar \Gamma \left(\frac{\Omega_0}{2\Delta_0} \right)^2 \frac{dR(\rho_j)}{d\rho_j} \sum_{m \neq j} R(\rho_m) \frac{\cos[k_0(r_{jm} - z_{jm}) - \ell\phi_{jm}]}{k_0 r_{jm}} \hat{\mathbf{u}}_\rho \\ &+ \ell \hbar \Gamma \left(\frac{\Omega_0}{2\Delta_0} \right)^2 \frac{R(\rho_j)}{\rho_j} \sum_{m \neq j} R(\rho_m) \frac{\sin[k_0(r_{jm} - z_{jm}) - \ell\phi_{jm}]}{k_0 r_{jm}} \hat{\mathbf{u}}_\phi + \mathbf{F}_{Lj}, \end{aligned} \quad (\text{B7})$$

with $\phi_{jm} = \phi_j - \phi_m$. The first term is due to the collective momentum recoil, weighted by the radial profile of the pump field. The second term is a collective radial force, due to variation of the radial profile of the pump. Notice that $dR(\rho_j)/d\rho_j = R(\rho_j)[\ell/\rho_j - 2\rho_j/w^2]$. The third term is the collective azimuthal force, due to the winging phase of the OAM pump.

APPENDIX C: DERIVATION OF EIGENVALUES OF EQ. (53)

The equations

$$\ddot{\phi}_j = \sum_{m=1}^N G(\phi_j - \phi_m) \quad (\text{C1})$$

with $j = 1, \dots, N$ have an equilibrium with $\phi_j = \phi_j^{(0)}$ such that

$$\sum_m G(\phi_j^{(0)} - \phi_m^{(0)}) = 0 \quad (\text{C2})$$

and $\dot{\phi}_j = 0$. Let us perturb the equilibrium with $\phi_j(t) = \phi_j^{(0)} + \delta\phi_j(t)$, with $\delta\phi_j \ll \phi_j^{(0)}$, and

$$\delta\ddot{\phi}_j = - \sum_{m=1}^N K(\phi_j^{(0)} - \phi_m^{(0)}) (\delta\phi_j - \delta\phi_m), \quad (\text{C3})$$

where

$$K(x) = - \frac{d}{dx} G(x) = \frac{d^2}{dx^2} V(x). \quad (\text{C4})$$

The first term on the right-hand side of Eq. (C3) is zero since

$$\begin{aligned} \sum_{m=1}^N K(\phi_j^{(0)} - \phi_m^{(0)}) &\rightarrow \frac{N}{2\pi} \int_0^{2\pi} d\phi' K(\phi - \phi') \\ &= - \frac{N}{2\pi} \int_\phi^{\phi+2\pi} dx \frac{d}{dx} G(x) \\ &= \frac{N}{2\pi} [G(\phi + 2\pi) - G(\phi)] = 0, \end{aligned} \quad (\text{C5})$$

and because $G(x)$ is periodic in $(0, 2\pi)$. The linear stability is governed by the equations

$$\delta\ddot{\phi}_j = \sum_{m=1}^N K(\phi_j^{(0)} - \phi_m^{(0)}) \delta\phi_m. \quad (\text{C6})$$

We write the potential $V(x)$ as

$$V(x) = - \frac{1}{2\rho'q(x)} (e^{-2i\rho'q(x)+i\ell x} + \text{c.c.}) = \alpha(x) e^{i\ell x} + \text{c.c.}, \quad (\text{C7})$$

where

$$\alpha(x) = - \frac{e^{-2i\rho'q(x)}}{2\rho'q(x)}, \quad (\text{C8})$$

so that

$$\begin{aligned} K(x) &= V''(x) = [\alpha''(x) + 2i\ell\alpha'(x) - \ell^2\alpha(x)] e^{i\ell x} + \text{c.c.} \\ &= \gamma(x) e^{i\ell x} + \text{c.c.} \end{aligned} \quad (\text{C9})$$

Introducing the linearized n th harmonic azimuthal bunching as

$$\delta\Phi_n(t) = \frac{1}{N} \sum_j e^{-in\phi_j^{(0)}} \delta\phi_j(t), \quad (\text{C10})$$

from Eqs. (C6) and (C9) it follows that

$$\begin{aligned} \delta\dot{\Phi}_n &= \frac{1}{N} \sum_j e^{-i(n-\ell)\phi_j^{(0)}} \sum_m \gamma(\phi_j^{(0)} - \phi_m^{(0)}) e^{-i\ell\phi_m^{(0)}} \delta\phi_m \\ &+ \frac{1}{N} \sum_j e^{-i(n+\ell)\phi_j^{(0)}} \sum_m \gamma^*(\phi_j^{(0)} - \phi_m^{(0)}) e^{i\ell\phi_m^{(0)}} \delta\phi_m. \end{aligned} \quad (\text{C11})$$

We define

$$F_m^n = \sum_j \gamma(\phi_j^{(0)} - \phi_m^{(0)}) e^{-i(n-\ell)\phi_j^{(0)}}, \quad (\text{C12})$$

$$G_m^n = \sum_j \gamma^*(\phi_j^{(0)} - \phi_m^{(0)}) e^{-i(n+\ell)\phi_j^{(0)}}, \quad (\text{C13})$$

so that

$$\delta\ddot{\Phi}_n = \frac{1}{N} \sum_m F_m^n e^{-i\ell\phi_m^{(0)}} \delta\phi_m + \frac{1}{N} \sum_m G_m^n e^{i\ell\phi_m^{(0)}} \delta\phi_m. \quad (\text{C14})$$

In order to determine F_m^n and G_m^n , we transform the sums over j into integrals considering $\phi_j^{(0)}$ and $\phi_m^{(0)}$ as continuous variables with uniform distribution:

$$F^n(\phi) = \frac{N}{2\pi} \int_0^{2\pi} \gamma(\phi' - \phi) e^{-i(n-\ell)\phi'} d\phi', \quad (\text{C15})$$

$$G^n(\phi) = \frac{N}{2\pi} \int_0^{2\pi} \gamma^*(\phi' - \phi) e^{-i(n+\ell)\phi'} d\phi'. \quad (\text{C16})$$

Changing the integration variable into $x = \phi' - \phi$, we obtain

$$\begin{aligned} F^n(\phi) &= e^{-i(n-\ell)\phi} \frac{N}{2\pi} \int_0^{2\pi} \gamma(x) e^{-i(n-\ell)x} dx \\ &= N\gamma_{n-\ell} e^{-i(n-\ell)\phi}, \end{aligned} \quad (\text{C17})$$

$$\begin{aligned} G^n(\phi) &= e^{-i(n+\ell)\phi} \frac{N}{2\pi} \int_0^{2\pi} \gamma^*(x) e^{-i(n+\ell)x} dx \\ &= N\gamma_{-(n+\ell)}^* e^{-i(n+\ell)\phi}, \end{aligned} \quad (\text{C18})$$

where

$$\gamma_k = \frac{1}{2\pi} \int_0^{2\pi} \gamma(x) e^{-ikx} dx \quad (\text{C19})$$

is independent on ϕ . Hence, we obtain in the discrete form

$$F_m^n = N\gamma_{n-\ell} e^{-i(n-\ell)\phi_m^{(0)}}, \quad (\text{C20})$$

$$G_m^n = N\gamma_{-(n+\ell)}^* e^{-i(n+\ell)\phi_m^{(0)}}, \quad (\text{C21})$$

and

$$\delta\ddot{\Phi}_n = N[\gamma_{n-\ell} + \gamma_{-(n+\ell)}^*] \delta\Phi_n. \quad (\text{C22})$$

The coefficient γ_k is

$$\gamma_k = \frac{1}{2\pi} \int_0^{2\pi} [\alpha''(x) + 2i\ell\alpha'(x) - \ell^2\alpha(x)] e^{-ikx} dx. \quad (\text{C23})$$

By integrating by parts we obtain

$$\gamma_k = (k + \ell)^2 v_k, \quad (\text{C24})$$

where

$$v_k = -\frac{1}{2\pi} \int_0^{2\pi} \alpha(x) e^{-ikx} dx. \quad (\text{C25})$$

Assuming $\Phi_n(t) \propto e^{\lambda_n t}$, then

$$\lambda_n^2 = N[\gamma_{n-\ell} + \gamma_{-(n+\ell)}^*]. \quad (\text{C26})$$

Using Eqs. (C24), (C25), and (C7), we obtain

$$\lambda_n = \pm n\sqrt{N} \sqrt{v_{n-\ell} + v_{-(n+\ell)}^*} = \pm in\sqrt{NV_n} \quad (\text{C27})$$

where

$$V_n = \frac{1}{2\pi} \int_0^{2\pi} V(x) e^{-inx} dx. \quad (\text{C28})$$

The growth rate and the frequency for the n th bunching are $|\text{Re}(\lambda_n)|$ and $\text{Im}(\lambda_n)$, where the last expression refers to the solution with $\text{Re}(\lambda_n) > 0$.

-
- [1] R. Bonifacio and L. D. S. Souza, Collective atomic recoil laser (Carl) optical gain without inversion by collective atomic recoil and self-bunching of two-level atoms, *Nucl. Instrum. Methods Phys. Res.* **341**, 360 (1994).
- [2] R. Bonifacio, L. De Salvo, L. M. Narducci, and E. J. D'Angelo, Exponential gain and self-bunching in a collective atomic recoil laser, *Phys. Rev. A* **50**, 1716 (1994).
- [3] D. Kruse, C. von Cube, C. Zimmermann, and P. W. Courteille, Observation of Lasing Mediated by Collective Atomic Recoil, *Phys. Rev. Lett.* **91**, 183601 (2003).
- [4] S. Slama, S. Bux, G. Krenz, C. Zimmermann, and P. W. Courteille, Superradiant Rayleigh scattering and Collective Atomic Recoil Lasing in a Ring Cavity, *Phys. Rev. Lett.* **98**, 053603 (2007).
- [5] R. A. Beth, Direct detection of the angular momentum of light, *Phys. Rev.* **48**, 471 (1935).
- [6] L. Allen, M. W. Beijersbergen, R. J. C. Spreeuw, and J. P. Woerdman, Orbital angular momentum of light and the transformation of Laguerre-Gaussian laser modes, *Phys. Rev. A* **45**, 8185 (1992).
- [7] M. Babiker, W. L. Power, and L. Allen, Light-Induced Torque on Moving Atoms, *Phys. Rev. Lett.* **73**, 1239 (1994).
- [8] S. Franke-Arnold, Optical angular momentum and atoms, *Phil. Trans. R. Soc. A* **375**, 20150435 (2017).
- [9] G. Robb, Superradiant exchange of orbital angular momentum between light and cold atoms, *Phys. Rev. A* **85**, 023426 (2012).
- [10] G. Robb, Collective exchange of orbital angular momentum between cold atoms and light, *AIP Conf. Proc.* **1421**, 93 (2012).
- [11] M. E. Tasgin, O. E. Müstecaplıođlu, and L. You, Creation of a vortex in a Bose-Einstein condensate by superradiant scattering, *Phys. Rev. A* **84**, 063628 (2011).
- [12] P. Das, M. E. Tasgin, and Á. E. Müstecaplıođlu, Collectively induced many-vortices topology via rotatory Dicke quantum phase transition, *New J. Phys.* **18**, 093022 (2016).
- [13] R. Ayllon, J. T. Mendonça, A. T. Gisbert, N. Piovela, and G. R. M. Robb, Multimode collective scattering of light in free space by a cold atomic gas, *Phys. Rev. A* **100**, 023630 (2019).
- [14] A. T. Gisbert and N. Piovela, Multimode collective atomic recoil lasing in free space, *Atoms* **8**, 93 (2020).
- [15] L. Amico, A. Osterloh, and F. Cataliotti, Quantum Many Particle Systems in Ring-Shaped Optical Lattices, *Phys. Rev. Lett.* **95**, 063201 (2005).

- [16] S. Franke-Arnold, J. Leach, M. J. Padgett, V. E. Lembessis, D. Ellinas, A. J. Wright, J. M. Girkin, P. Öhberg, and A. S. Arnold, Optical ferris wheel for ultracold atoms, *Opt. Express* **15**, 8619 (2007).
- [17] A. M. Yao and M. J. Padgett, Orbital angular momentum: Origins, behavior and applications, *Adv. Opt. Photonics* **3**, 161 (2011).
- [18] G. Robb, N. Piovella, and R. Bonifacio, The semiclassical and quantum regimes of super-radiant light scattering from a Bose-Einstein condensate, *J. Opt. B* **7**, 93 (2005).
- [19] R. Bachelard, N. Piovella, and S. Gupta, Slow dynamics and subdiffusion in a non-Hamiltonian system with long-range forces, *Phys. Rev. E* **99**, 010104(R) (2019).